Analytical Model of Soil-Water Characteristics Considering the Effect of Air Entrapment

Pan Chen[1]; Changfu Wei[2]; and Tiantian Ma[3]

Abstract: Based on experimental data and the flow property analysis of the drying-wetting process of fluids under a microscope, a theoretical model is developed to consider the effect of air entrapment in the soil-water retention constitutive relationship. The effect of hysteresis on the fluid flow is considered by introducing an integrated capillary hysteretic model. There are only three conditions needed in the new model, i.e., the primary drying boundary curve, the main wetting boundary curve, and one point in the main hysteretic loop. Furthermore, as long as the previously experienced maximum matric suction in the porous medium is given, the model is capable of simulating changes of the soil-water state with the effect of air entrapment undergoing an arbitrary change of matric suction. By comparing the predictive curves with measured data from the literature, it is shown that the effects of air entrapment and capillary hysteresis are significant on the soil-water retention relationships. The model with the effects of capillary hysteresis and air entrapment should be taken into account in the soil-water relationship in order to accurately predict soil-moisture states in porous media. **DOI: 10.1061/(ASCE)GM.1943-5622.0000462.**

Introduction

In general, a geomaterial (e.g., a soil) cannot be fully saturated through a wetting process because of air entrapment. During a wetting process, because of the local heterogeneity of the soil, the water tends to fill smaller pores first and then larger pores. Hence, the passageway of the air in the larger pores can be blocked when the degree of saturation is high, and some amount of pore air is trapped in the soil. The trapped air exists in the soil as air bulbs, which are surrounded by the wetting fluid (i.e., pore water) in the porous medium (Bond and Collis-George 1981). Air entrapment can significantly influence the hydraulic conductivity of soils (Stonestrom and Rubin 1989; Seymour 2000; Hammecker et al. 2003). The effect of capillary hysteresis and air entrapment have an important influence on the resilient modulus, stress-strain relationship, and shear strength of unsaturated soils (Khoury et al. 2012; Liu and Muraleetharan 2012; Chen et al. 2013). Similar to the effect of air entrapment, residual nonaqueous phase liquids (NAPLs) can also be trapped in multiphase porous medium systems. The quality of groundwater is affected in the long term by the trapped or residual NAPLs because the fluids gradually dissolve into the surrounding porous water and seep into the groundwater (Miller et al. 1990; Lenhard et al. 2004). Organic compounds and other solvents can cause contamination of the aquifer over long periods of time because of their low solubility (Van Geel and Roy 2002). The distribution of the trapped NAPL is important in the assessment of the contamination source and the effective remediation of the contaminated site (Van Geel and Sykes 1997; Hilpert et al. 2000). Under fluctuating water table conditions, entrapment of light NAPLs (LNAPLs) has a significant effect on the LNAPL distribution in unsaturated sand that is contaminated as a result of a LNAPL spill (Van Geel and Sykes 1997).

The amount of trapped air depends on the minimal degree of saturation, or the highest matric suction, that the soil experiences. Sharma and Mohamed (2003) demonstrated that the content of trapped air largely depends on the reversal degree of saturation of the soil during a drying-wetting cycle. The reversal degree of saturation is defined as the degree of saturation at the turning point of the drying-wetting cycle. Sharma and Mohamed (2003) also demonstrated that the functional relationship between the content of trapped air and the reversal degree of saturation is nonlinear, and that the content of trapped air is changed with drying-wetting cycles. Trapped air significantly influences the soil-water retention relationships at a high degree of the saturation state, and the amount of trapped air changes monotonically with the water content in soils (Stonestrom and Rubin 1989). The formula between the amount of trapped air and the reversal degree of saturation has been previously developed (Land 1968; Lenhard and Parker 1987; Gerhard et al. 1998). The maximum residual degree of saturation of NAPL is related to the particle-size distribution; the properties of the fluid-solid interface, especially wettability; and the properties of various fluids in a porous medium (including the viscosity ratio, interfacial tension, and density difference) (Stegemeier 1977).

The effects of air entrapment should be taken into account in the soil-water retention relationship in order to accurately predict the change of the soil-moisture state in a porous medium. Although many new models have been developed to describe the soil-water retention relationship (Krishnapillai and Ravichandran 2012; Noh et al. 2012), very few models include the effect of capillary hysteresis and air entrapment in the saturation-capillary pressure relationship (Van Geel and Sykes 1997). Some models have been developed to describe the relationships of hysteretic saturation-capillary pressure,

[1]Assistant Professor, State Key Laboratory of Geomechanics and Geotechnical Engineering, Institute of Rock and Soil Mechanics, Chinese Academy of Sciences, Wuhan, Hubei 430071, P.R. China (corresponding author). E-mail: pchen@whrsm.ac.cn

[2]Professor, State Key Laboratory of Geomechanics and Geotechnical Engineering, Institute of Rock and Soil Mechanics, Chinese Academy of Sciences, Wuhan, Hubei 430071, P.R. China. E-mail: cfwei@whrsm.ac.cn

[3]Assistant Professor, State Key Laboratory of Geomechanics and Geotechnical Engineering, Institute of Rock and Soil Mechanics, Chinese Academy of Sciences, Wuhan, Hubei 430071, P.R. China. E-mail: ttma@whrsm.ac.cn

Note. This manuscript was submitted on April 9, 2014; approved on October 22, 2014; published online on November 11, 2014. Discussion period open until April 11, 2015; separate discussions must be submitted for individual papers. This paper is part of the ***International Journal of Geomechanics***, © ASCE, ISSN 1532-3641/04014102(10)/$25.00.

in which the effect of entrapment air and oil phase during the wetting process was considered (Parker and Lenhard 1987; Lenhard and Parker 1987). The content of trapped nonwetting fluid was obtained by extending the method developed by Land (1968), in which a linearly interpolated method was used. Although this method can decrease the number of computations and amount of parametric acquisition, the parameters of the model increase because the effect of trapped air is considered. Moreover, the scaling approach, which was developed by Lenhard and Parker (1987), essentially assumed that the capillary tube model is valid; however, it neglected the effect of the contact angle (Kechavarzi et al. 2005). Variation of the contact angle causes significant hysteresis in the soil-moisture state (Likos and Lu 2002). Steffy et al. (1998) improved the scaled inhibition pressure-saturation relationships by incorporating a correction for contact angle hysteresis and surface roughness. Gerhard and Kueper (2003) also constructed a constitutive model considering the hysteretic effect and entrapped dense NAPLs (DNAPLs) during the infiltration and redistribution process.

This paper focuses on analyzing the soil-water distribution and pore pressure change as a result of entrapped air in porous media under an arbitrary change of the degree of saturation or matric suction conditions. First, based on analysis of the experimental data, a theoretical model is developed to consider the effect of entrapped air in unsaturated soils during the drying-wetting cycles. Then, the new soil-water characteristic relationship model is used to simulate the changes of the degree of saturation and pore pressure. Finally, the predictive curves are compared with the experimental data from the literature to validate the new model.

Theoretical Formation

Conceptual Model

Capillary hysteresis commonly occurs in unsaturated porous media with the increase and decrease of water content. The mechanism of the hysteresis effect has been the focus of previous research and has been explained by many theoretical models. The research results from the literature have offered conclusions to explain the mechanism of capillary hysteresis (Likos and Lu 2004). Based on the mechanism research about capillary hysteresis, some models have been developed to describe the change of the soil-moisture state with the effect of capillary hysteresis in porous media (Miller et al. 2008; Nuth and Laloui 2008; Tan et al. 2009). In fact, the entrapped effect of air and NAPL is one of the main reasons for capillary hysteresis. However, the effect of air entrapment has not been considered in these models. Hence, these soil-water retention curve (SWRC) models are imprecise when modeling the flow phenomenon of air entrapped in the pores of unsaturated soils. Therefore, in this study a new model is developed to consider the effect of air entrapment in the unsaturated seepage process that experiences drying-wetting histories.

Wardlaw and Taylor (1976) carried out mercury injection and withdrawal tests on various rocks. Mercury is a nonwetting liquid in the gas-mercury system because the wet potential of mercury is smaller than that of gas. Wardlaw and Taylor (1976) found that the content of entrapped mercury is closely related to the degree of saturation of mercury at the transform point from the intrusion curve to the extrusion curve. A similar result was observed in unsaturated soils by Stonestrom and Rubin (1989). Here, two assumptions can be put forward based on the aforementioned phenomenon that occurred during the drying and rewetting experiments. One is that the content of air entrapment only depends on the previously experienced maximum matric suction (or at the lowest degree of saturation state). The other is that the scanning curves of the soil-moisture retention curve can be uniquely determined by the closed hysteresis circles, depending upon the previously experienced maximum matric suction. Also, the slope of the scanning curves is not affected by the content of trapped air. The rationality of the two assumptions can be well explained from the microporosity scale. In order to clearly explain the mechanism, schematics are given in Fig. 1. In the beginning, the porous media are fully saturated. Based on the capillary tubes bundle theory, one matric suction s_{ci} corresponds to a certain equivalent porosity radius r_i. Three different equivalent pore radii are shown in Fig. 1. The aqueous phase liquid (e.g., water phase) is expelled from the pores with equivalent pore radii larger than or equal to r_1, corresponding to the matric suction value, s_{c1}. However, the aqueous phase liquid can be still stored in pores with radius smaller than r_1, as shown in Fig. 1(a). The drying process will further continue when the matric suction increases to s_{c2}. The wetting liquid will flow out from all pores with equivalent pore radii larger than r_2, as shown in Fig. 1(b). In the same way, the aqueous phase liquid in pores with radii larger than r_i can be expelled under the matric suction s_{ci} condition. The drying process will finish when the aqueous phase liquid stops discharging at matric suction s_{ci}. Furthermore, pores with equivalent pore radius r_i start to absorb moisture if matric suction s_{ci} decreases gradually, and the other pores are not affected at matric suction s_{ci} during the drying and wetting process. Here, s_{ci} can be referred to as the previously experienced maximum matric suction. Hence, the first assumption that the content of air entrapment only depends on the previously experienced maximum matric suction is reasonable. Compared with the volume of one porous medium, the volume of air entrapment is rather small within the change of matric suction at each step. In reality, the connectivity among pores is not very strong. Therefore, the effect of air entrapment is the same in the drying and wetting process when the

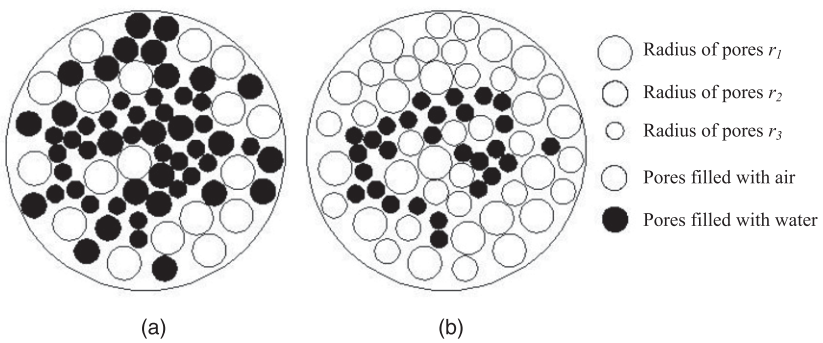

Fig. 1. Schematics of the draining progress of porous water in porous media: (a) under matric suction s_{c1}; (b) under matric suction s_{c2}

Int. J. Geomech.

matric suction increases or decreases within the range of s_{ci} (Wardlaw and Taylor 1976). Also, the effect of air entrapment is not significant in relation to water flow in pores smaller than r_i when the matric suction continues to increase (Wardlaw and Taylor 1976). Consequently, the second assumption is rational.

The primary drying curve (IDC), main drying curve (MDC), and main wetting curve (MWC) are generally called the boundary curves of the SWRC, as shown in Fig. 2. The difference in the degree of saturation between the IDC and MWC at zero matric suction is the maximum degree of saturation of entrapped air, $S_{r\max}^{\text{trap}}$. The scanning curves are included in the boundary curves. These scanning curves can be divided into two types. One type is included in the closed loop that is constituted of the MWC and MDC. The other is included between the IDC and MDC. The first type of scanning curves can be predicted by constructing a capillary hysteresis model, such as the model of capillary hysteresis [i.e., the internal state variable hysteresis (ISVH) model] developed by Wei and Dewoolkar (2006). The secondary type of scanning curves is affected by the effect of air entrapment. A new model should be developed to consider the effect of air entrapment for the change of the soil-water state.

Based on the two previous assumptions the change rate of water content along the drying or wetting scanning curves starting from the IDC can be determined, as long as the previously experienced maximum matric suction or the corresponding degree of saturation is given. The details of this method are illustrated in Fig. 2. The matric suction is $s_{ci}^{\max}$ at Point B, where the porous media start to absorb water after the drying process. A closed hysteretic loop (ADBC) forms after the drying-wetting cycle. The distance between Point O at the full saturation state and Point A is called the degree of saturation of entrapped air, S_{ri}^{trap}. The closed hysteretic loop (ADBC) can be predicted according to the following method with the effect of air entrapment. First, Point B is translated left and intersects with Curve MDC at Point F ($s_c^F = s_{ci}^{\max}$). The length of BF is equal to that of AE from the geometric relationship. Under the decrement of matric suction starting from Point B ($s_{ci}^{\max}$), the soil-water state reaches Point C (s_c^C). The water content at Point C can be determined by using the translating method. From Point F, the matric suction also changes the same increment to Point G. Then, the change of water content and slope of the scanning curve can be modeled through the ISVH model in the main hysteretic loop (MHL). The ISVH model is based on a rigid thermodynamic-consistent framework, which uses the boundary surface plasticity theory to simulate the hysteretic behavior of the soil-moisture state (Wei and Dewoolkar 2006). The real water content is gained by translating right of the length of BF, and the slope is the same as the scanning curve in the MHL. In the same way, the change of water content can also be determined by the drying path from Point H to Point F when the matric suction at Point D (s_c^D) is increased to Point B. The state of the water content under any change of matric suction is completely determined through the method. Hence, the closed hysteretic loop (ADBC) can be predicted. The other scanning curves from the saturated state to the unsaturated state can also be modeled using the same method. Based on the two previous assumptions, the wetting scanning curve (BCA) can actually be coincident with the scanning curve (FGE) by the translational method, and the drying scanning curve (ADB) can be obtained by paralleling the scanning curve (EHF). If the drying or wetting transform process comes out in the loop (ADBC), the loop related to the previously experienced matric suction $s_{ci}^{\max}$ is first paralleled into the MHL (FGEH), and the change of water content can be predicted in the loop (FGHE). Then, these higher-order scanning curves can be obtained in the loop (ADBC). The hysteretic loop (ADBC) needs to be renewed once the matric suction increases to the one larger than $s_{ci}^{\max}$ at Point I during the drying process. The change of water content needs to be determined in the new hysteretic loop, depending on matric suction s_c^I at Point I. The previously experienced maximum matric suction is also renewed ($s_{ci}^{\max} = s_c^I$). Then, the translating method is used again to give the actual soil-water state under repeated hydraulic conditions.

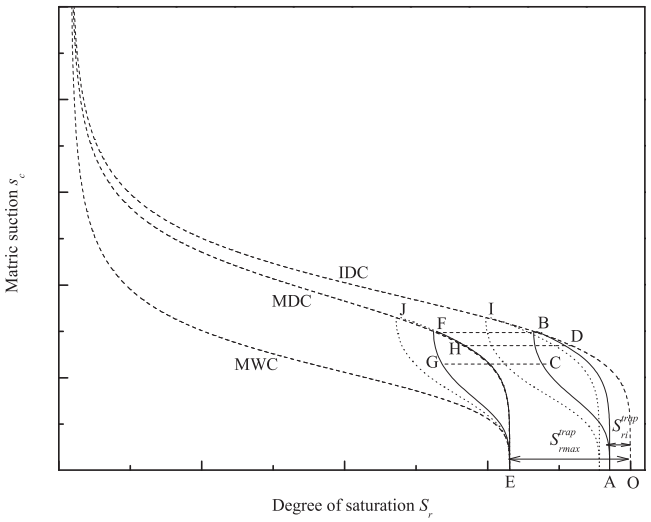

Fig. 2. Schematics of the theoretical model for the SWRC

Mathematical Description of the Theoretical Model

Prediction of Soil-Water Retention Curves with the Effect of Air Entrapment

Based on the aforementioned mechanical analysis, mathematical formulas can be obtained to predict the scanning curves. The hysteretic circle (ADBC), which includes the secondary scanning curves, is up to the maximum matric suction that the porous media have experienced along the IDC, as shown in Fig. 2. The soil-water state of one Point B can be described by $s_{ci}^{\max}$ and S_{ri}^{IDC} on the IDC. Point B ($s_{ci}^{\max}$, S_{ri}^{IDC}) is then translated left to another Point F ($s_{ci}^{\max}$, S_{ri}^{MDC}) on the MDC. Once the change of matric suction is given in the MHL, the hysteretic circle (EHFG) in the space between the wetting (FGE) and drying (EHF) curves will be determined uniquely.

The translational change of degree of saturation of the water phase from Point B on the IDC to Point F on the MDC is computed as

$$S_{ri}^{\text{MDC}} = S_{ri}^{\text{IDC}} - \left(S_{r\max}^{\text{trap}} - S_r^{\text{trap}}\right) \tag{1}$$

where S_{ri}^{MDC} = degree of saturation of the water phase on the MDC corresponding to translating left the maximum matric suction point into the main hysteresis loop; S_{ri}^{IDC} = reversal degree of saturation of the water phase on the IDC corresponding to transition point $s_{ci}^{\max}$; S_r^{trap} = degree of saturation of air entrapment in relation to $s_{ci}^{\max}$; and $S_{r\max}^{\text{trap}}$ = maximum content of air entrapment between the IDC and MWC.

Loop ADBC can be translated left into the MHL and coincides with Loop EHFG. Assuming the increment of matric suction, $\dot{s}_c$, the change degree of saturation in the MHL, $\dot{S}_r^W$, can be computed as follows:

$$\dot{S}_r^W = -\dot{s}_c / K_p \tag{2}$$

where K_p = slope of the scanning curve, in which the variable is a function of S_r^W, s_c, and $\hat{n}$; S_r^W and s_c = present degree of saturation

and matric suction in the MHL, respectively; and $\hat{n}$ = direction of the hydraulic path, in which its value is −1 or 1. For the wetting path, $\hat{n} = -1$, and for the drying path, $\hat{n} = 1$. Here, K_p is given as follows:

$$K_p = \overline{K_p} + d\left|s_c - \overline{s_c}\right| \Big/ \left(r - \left|s_c - \overline{s_c}\right|\right) \tag{3}$$

where d = fit parameter, which is an additional parameter used to describe all of the scanning curves in the main hysteretic circle; the matric suctions at the main drying and wetting boundary curves are expressed by $\overline{s}_c = \kappa_D(S_r^W)$ and $\overline{s}_c = \kappa_W(S_r^W)$, respectively; r = difference of matric suction between the main boundary curves when the soil-water state is at the degree of saturation S_r^W, $r = \kappa_D(S_r^W) - \kappa_W(S_r^W)$; and $\overline{K}_p$ and $\overline{s}_c(S_r^W, \hat{n})$ = slope and matric suction of the main drying and wetting boundary curves, respectively, which are obtained for the drying path ($\hat{n} = 1$) and wetting path ($\hat{n} = -1$) as follows:

$$\overline{s}_c\left(S_r^W, 1\right) = \kappa_D\left(S_r^W\right), \quad \overline{K}_p\left(S_r^W, 1\right) = d\kappa_D\left(S_r^W\right) \Big/ dS_r^W \tag{4a}$$

$$\overline{s}_c\left(S_r^W, -1\right) = \kappa_W\left(S_r^W\right), \quad \overline{K}_p\left(S_r^W, -1\right) = d\kappa_W\left(S_r^W\right) \Big/ dS_r^W \tag{4b}$$

Corresponding to the small increment of matric suction $\dot{s}_c$, the degree of saturation S_r^{MHL} in the MHL is given as follows:

$$S_r^{\mathrm{MHL}} = S_{ro}^{\mathrm{MHL}} + \dot{S}_r^W \tag{5}$$

where S_{ro}^{MHL} = degree of saturation at matric suction s_c. The actual degree of saturation S_r^W is obtained by the transition method at matric suction $(s_c + \dot{s}_c)$

$$S_r^W = S_r^{\mathrm{MHL}} + S_{r\max}^{\mathrm{trap}} - S_r^{\mathrm{trap}} \tag{6}$$

In general, the boundary curves are needed in the theoretical model to compute the change of the degree of saturation under any change of the matric suction condition. The IDC and MWC can be first fitted by a soil-water retention model. Here, the soil-water retention curve model developed by Feng and Fredlund (1999) is adopted as the boundary curve equation

$$s_c = b\left[\left(S_r^i - S_r^W\right) \Big/ \left(S_r^W - S_r^{\mathrm{irr}}\right)\right]^{1/a} \tag{7}$$

where $S_r^i = 1.0$ (for the IDC) and $S_r^i = S_r^{\mathrm{MWC}}$ (for the MWC); a and b = empirical parameters obtained from fitting the experimental data; S_r^{irr} = residual degree of saturation of the water phase; and S_r^{MWC} = degree of saturation when the matric suction is zero on the MWC. There is one constraint needed to be satisfied as follows:

$$S_r^{\mathrm{MWC}} + S_{r\max}^{\mathrm{trap}} = 1.0 \tag{8}$$

and parameters of the MDC are also obtained by Eq. (7). The parameters will be excessive in the theoretical model if the fitting parameters for the MDC are adopted. Hence, a new simplified method is developed to predict the MDC in the subsequent section.

Predictive Formula of the MDC

The content of air entrapment is related to maximum matric suction $s_{ci}^{\max}$, which previously is obtained from the unsaturated porous media. The degree of saturation on the MDC (S_{ri}^{MDC}) according to $s_{ci}^{\max}$ can be obtained by translating left the point ($s_{ci}^{\max}$, S_{ri}^{IDC}) on the IDC to the MDC. The formula can be gained from the geometry as

$$S_r^{\mathrm{trap}} = S_{r\max}^{\mathrm{trap}} - \left(S_{ri}^{\mathrm{IDC}} - S_{ri}^{\mathrm{MDC}}\right) \tag{9}$$

The degree of saturation of entrapped air S_r^{trap} will always retain a constant value as long as the change of matric suction is not larger than the previously experienced maximum matric suction $s_{ci}^{\max}$. Eq. (9) can be rewritten as follows:

$$S_{ri}^{\mathrm{MDC}} = S_{ri}^{\mathrm{IDC}} - \left(S_{r\max}^{\mathrm{trap}} - S_r^{\mathrm{trap}}\right) \tag{10}$$

Thus, as long as the degree of saturation of entrapped air S_r^{trap} can be obtained according to $s_{ci}^{\max}$ or S_{ri}^{IDC}, the reversal degree of saturation on the MDC can be obtained using Eq. (10). If the matric suction continues to increase along the IDC, $s_{ci}^{\max}$ would be renewed, and the degree of saturation of entrapped air S_r^{trap} should be solved again. In the same way, the change of degree of saturation can be predicted along the main drying path by the IDC and the maximum degree of saturation of entrapped air $S_{r\max}^{\mathrm{trap}}$ using Eq. (10). Hence, the relationship between S_r^{trap} and $s_{ci}^{\max}$ or S_{ri}^{IDC} will be discussed in the subsequent section.

Relationship between S_r^{trap} and S_r^{Wt}: Modified Relationship between S_r^{trap} and S_r^{Wt}

The effect of entrapped nonwetting fluid was considered by Gerhard et al. (1998) in order to explore the law of the DNAPL flow in porous media. An empirical equation was developed based on the measured data between the content of the entrapped DNAPL and the degree of saturation of the water phase. The equation is given as follows:

$$S_r^{\mathrm{trap}} = S_{r\max}^{\mathrm{trap}}\left(1 - S_r^{Wt}\right) \tag{11}$$

where S_r^{trap} = degree of saturation of entrapped DNAPL; $S_{r\max}^{\mathrm{trap}}$ = maximum degree of saturation of entrapped DNAPL; and S_r^{Wt} = reversal degree of saturation of water when the hydraulic path begins to transform into a wetting path from a drying process, which is the degree of saturation according to the maximum matric suction that the porous media experience during the drying-wetting processes of the water content.

There are two restrictions that should be satisfied in Eq. (11)

$$S_r^{Wt} = 1.0, \quad S_r^{\mathrm{trap}} = 0.0 \tag{12a}$$

$$S_r^{Wt} = S_r^{\mathrm{irr}}, \quad S_r^{\mathrm{trap}} = S_{r\max}^{\mathrm{trap}} \tag{12b}$$

Eq. (12*a*) describes that the degree of saturation of entrapped DNAPL or air is zero when the porous media obtain a fully saturated state; Eq. (12*b*) describes that the degree of saturation of entrapped DNAPL or air is up to the maximum degree of saturation of entrapped DNAPL or air $S_{r\max}^{\mathrm{trap}}$ when the degree of saturation reaches the residual state with the degree of saturation S_r^{irr} in the porous media. Eq. (12*a*) can be obtained by Eq. (11). However, the restriction of Eq. (12*b*) is not yet satisfied in Eq. (11). To satisfy the restriction in Eq. (12*b*), Eq. (11) could be modified as follows:

$$S_r^{\mathrm{trap}} = S_{r\max}^{\mathrm{trap}}\left(1 - S_e^{Wt}\right) \tag{13}$$

The new relationship may be referred to as a modified Gerhard's model. Here, S_e^{Wt} is the effective reversal degree of saturation of water according to the previously experienced maximum matric suction. The effective degree of saturation can be defined as $S_e^{Wt} = (S_r^{Wt} - S_r^{\mathrm{irr}})/(1 - S_r^{\mathrm{irr}})$. The restrictions from Eqs. (12*a*) and (12*b*) can be satisfied automatically in Eq. (13). Although Eq. (11) is obtained from the flow test of organic fluids, the validity of the

modified Eq. (11) [i.e., Eq. (13)] is not confirmed in the two-phase flow for air and water in unsaturated soils. Hence, soil-water retention relationship tests have been done to verify the correctness of Eq. (13).

Relationship between S_r^{trap} and S_r^{Wt}: Verification of the Formula of the Content of Trapped Air

To verify Eq. (13), some experiments were done in the laboratory to measure the relationship between S_r^{trap} and S_r^{Wt} of unsaturated soils. The physical characteristics of the soils used in the tests are given in Table 1.

The samples were saturated by vacuum packaging after the soils were prepared in cutting rings. Then, one-step drying-wetting outflow tests were done in the flow tempe cell. One-step loading of the matric suction was imposed on the soil sample. The mass of the outflow water can be measured by a balance. The matric suction decreased to zero after the equilibrium state was reached during the drying process. Then, the wetting water test was performed. The difference was the content of entrapped air between the drainage mass of the water content and the absorption mass. The same soil sample was saturated once again after the one-step drying-wetting test was finished. Next, the step matric suction was loaded on the sample, and the drainage process of the soil began. The wetting was done as soon as the drying process reached its equilibrium state. In the same way, the drying-wetting tests were done as in the aforementioned method at each given matric suction. The matric suction steps for sand were 10, 30, 60, and 100 kPa. However, the steps for silt were 30, 60, 120, 240, and 290 kPa. The measured relationship between the transitional degree of saturation S_r^{Wt} and the content of entrapped air S_r^{trap} is shown in Fig. 3 for sand and silt, respectively. The predictive curves are also shown in Fig. 2 using Eqs. (11) and (13). Although a small discrepancy exists between the measured data and predictive results, the empirical equation can briefly describe the relationship between S_r^{Wt} and S_r^{trap}. Furthermore, the predictive curve is nearer the measured data using the modified equation than using Gerhard's equation. The modified equation is not only simple in form but it also automatically satisfies the restrictive conditions. Moreover, no additional parameters are introduced.

The modified relationship was verified using the measured data for the sand and silt. Although verification was not done on other soil types (e.g., clayey soils), the method adopted is feasible. However, the linear relationship may not be valid for other soil types, and a more complicated relationship can be developed to describe the relationship between S_r^{Wt} and S_r^{trap}. Then, the empirical equation can be used to reduce the parameters of the aforementioned new theoretical model. In this paper, the linear relationship of Eq. (13) will be used to predict the MDC with the effect of entrapped air. The degree of saturation of entrapped air S_r^{trap} has been obtained using Eq. (13). Hence, the MDC can be predicted by Eq. (10). That is, the MDC can be described by the IDC and S_{rmax}^{trap}, and no additional parameter is introduced into the new model to obtain the MDC.

Thus, the theoretical model has been developed. There are seven parameters needed to describe the change of water content under any change of matric suction conditon: S_r^{irr}, a^{IDC}, b^{IDC}, a^{MWC}, b^{MWC}, S_{rmax}^{trap} (or S_r^{MWC}), and d. Parameters S_r^{irr}, a^{IDC}, and b^{IDC} are obtained by fitting the IDC. Parameters a^{MWC} and b^{MWC} are obtained by fitting the MWCs. Parameter d can be gained by fitting one point or one scanning curve in the hysteretic circle made up of the MWC and MDC. A theoretical model has been developed, which can be called the simple ISVH-trap model. The new model considers the effect of air entrapment and capillary hysteresis on the liquid flow in porous media undergoing drying-wetting cycles. The new model can be adopted to describe the

Table 1. Physical Parameters of the Tested Material

USCS classification	Specific gravity, G_s	Dry density, ρ_d (g/cm^3)	Porosity, n	Grain analysis (%)		
				<0.005 mm	0.005–0.075 mm	>0.075 mm
SM	2.70	1.64	0.393	3.6	39.9	56.5
ML	2.71	1.72	0.391	5.2	76.3	18.5

Note: ML = low-plasticity silt; SM = silty sand; USCS = Unified Soil Classification System.

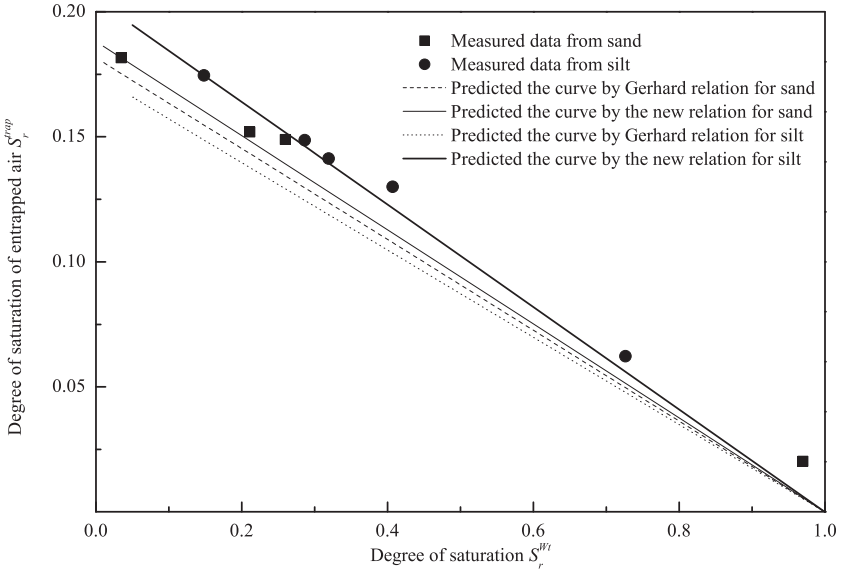

Fig. 3. Relationship between the degree of saturation of entrapment air and the degree of saturation from the experimental results

complicated changes of the soil-water state in porous media suffering any change in the history of the water content or matric suction.

Model Validation

Prediction of the MDC

The theoretical model needs to be verified using the measured data. Hence, the model was implemented into the program codes. The program was used to predict the soil-water retention curves and the results were compared with the experimental data from the literature. The experimental material was the mixed sand fractions, and the SWRC was measured using a dynamic method in a porous column developed by Poulovassilis (1970b). The IDC and MWC were fitted by Eq. (7) for the boundary curves in the literature. The physical parameters and model parameters are given in Table 2. The simple ISVH-trap model was used to predict the MDC. The predictive curve is compared with the measured data in Fig. 4, which shows good agreement between the measured data and predictive curve. No additional parameters were needed in the new model.

Prediction of the Soil-Water Retention Curves Undergoing Drying-Wetting Cycles

The experiment was carried out using sintered glass beads and their saturation with water under vacuum conditions. The static method was used to measure the SWRC in order to investigate the effect of trapped air on the hysteresis curves. More detail on this method can be found in Poulovassilis (1970a). The measured data are shown in Fig. 5. The MDC was first predicted by the new model. Then, one measured data point in the main hysteretic circle was used to calibrate parameter d. The parameters of the model are listed in Table 3. Furthermore, the new model was used to predict other scanning curves. These predictive curves are also shown in Fig. 5, compared with the measured data. As seen from Fig. 5, the predictive curves are coincident with the measured data with the effect of air entrapment. Hence, the new model is able to model the cycle change of the soil-moisture state in porous media under repeated increment and decrement of water content.

There is another example that validates the new model. The soil-water retention curve of fine silica sand was measured under static equilibrium in the laboratory by Mohamed and Sharma (2007). The porosity of the sand was 0.41, and the dry density of the sample was $1.61\ \mathrm{g/cm^3}$. The saturated sample was used before the tests were done. The maximum degree of saturation of entrapped air was 0.13. First, Eq. (7) was used for fitting the IDC and MWC. The model parameters are given in Table 4. Second, the MDC was predicted. To obtain parameter d, one scanning curve was used to calibrate the parameter. Finally, the new model was adopted to predict any change of water content and matric suction with the effect of air entrapment. The predictive curves and measured data are shown in Fig. 6, where a slight discrepancy is revealed between the measured data and the predictive MDC under low matric suction. The main reason for this is that some discrepancies appeared in the process of fitting the IDC using Eq. (7). The predicted drying scan curve is coincident with the measured data except for some discrepancies at the initial state. Once the matric suction is larger than the previously experienced maximum matric suction $s_{ci}^{\max} = 23.7$ cm, the soil-water state will move out of the hysteretic circle determined by $s_{ci}^{\max}$, and the change of water content and matric suction will be modeled in a new hysteretic circle determined by the new matric suction $s_{ci}^{\max}$. The scanning curves according to $s_{ci}^{\max} = 23.7$ cm between the IDC and MDC are also shown in Fig. 6, where the degree of saturation of entrapped air is approximately 7% according to $s_{ci}^{\max}$. The actual change of water content and matric suction is different from the boundary curves as

Table 2. Material Properties and Model Parameters of Mixed Sand

Parameter	Symbol	Quantity	Unit
Porosity	n_0	0.30	—
Residual degree of saturation	S_r^{irr}	11.6	Percentage
Maximum degree of saturation of entrapped air	$S_{r\max}^{\mathrm{trap}}$	14.7	Percentage
Model parameters for the simple ISVH-trap	b^{IDC}	30.37	cm
	b^{MWC}	22.49	cm
	a^{IDC}	6.55	—
	a^{MWC}	2.66	—

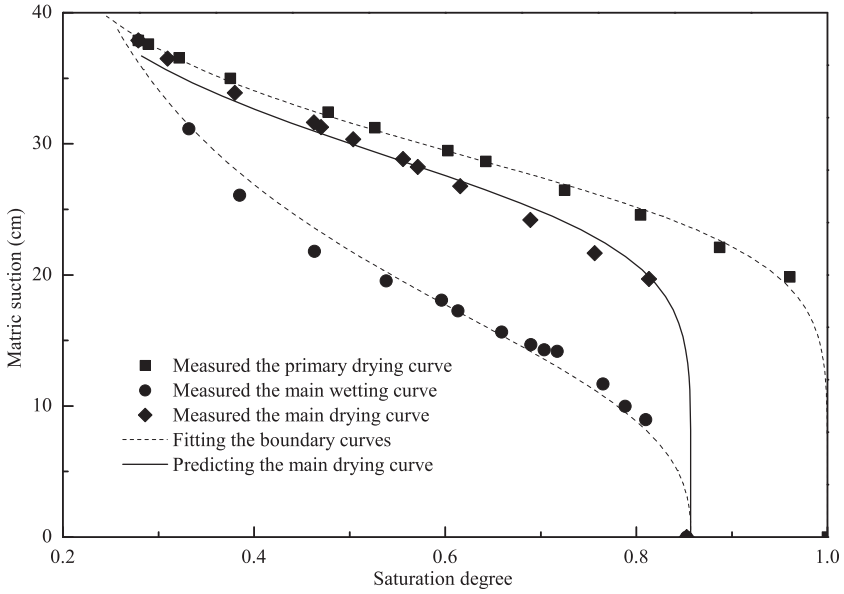

Fig. 4. Predictive curves and measured data of mixed sand fractions

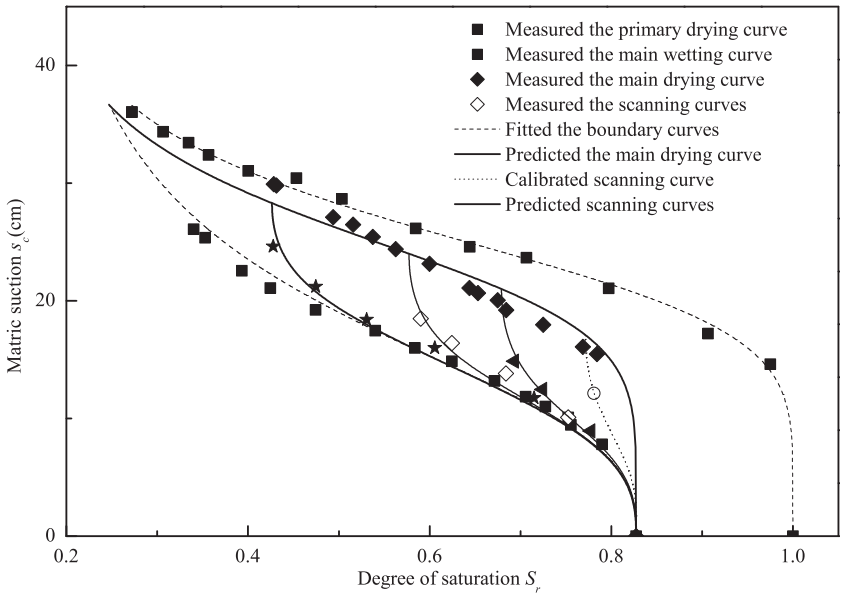

Fig. 5. Soil-water retention relationship of sand with the effect of capillary hysteresis and entrapped air subjected to wetting-drying cycles

Table 3. Material Properties and Model Parameters of Sand

Parameter	Symbol	Quantity	Unit
Porosity	n_0	0.33	—
Residual degree of saturation	S_r^{irr}	15.15	Percentage
Maximum degree of saturation of entrapped air	$S_{r\max}^{\text{trap}}$	17.27	Percentage
Model parameters for the simple ISVH-trap	b^{IDC}	26.43	cm
	b^{MWC}	19.44	cm
	a^{IDC}	5.52	—
	a^{MWC}	2.84	—
	d	500	cm

Table 4. Material Properties and Model Parameters of Fine Silica Sand

Parameter	Symbol	Quantity	Unit
Porosity	n_0	0.41	—
Residual degree of saturation	S_r^{irr}	13.7	Percentage
Maximum degree of saturation of entrapped air	$S_{r\max}^{\text{trap}}$	13.0	Percentage
Model parameters for the simple ISVH-trap	b^{IDC}	23.00	cm
	b^{MWC}	13.66	cm
	a^{IDC}	10.05	—
	a^{MWC}	7.25	—
	d	100	cm

a result of the effects of capillary hysteresis and air entrapment. Thus, the simple ISVH-trap model is efficient in simulating the soil-water retention relationship undergoing drying-wetting paths of water content. The hydraulic state of unsaturated soil (water content and matric suction) is significantly affected by the effect of entrapped air. Furthermore, the hydraulic and mechanical behavior of unsaturated soil will show some different properties under repeated changes of hydraulic paths. Hence, to predict the hydraulic and mechanical characteristics of unsaturated soil, the effect of entrapped air should be included in the unsaturated flow analysis.

The effect of air entrapment also exists in other porous media besides unsaturated soils, such as rocks. To explore the mechanism of air entrapment, mercury-injection and withdrawal cyclic tests were done by Wardlaw and Taylor (1976) using the Ruska mercury-injection capillary pressure apparatus, where mercury was a nonwetting liquid in an air-mercury two-phase flow system. Hence, a transform formula is needed as follows:

$$S_r^W = 1 - S_r^N \tag{14}$$

where S_r^W = degree of saturation of the wetting liquid; and S_r^N = degree of saturation of the nonwetting liquid. Here, S_r^W is the degree of saturation of air and S_r^N is the degree of saturation of mercury in the air-mercury flow system. The sample used was Midale dolomite from a Weyburn field in Saskatchewan, Canada. The porosity of the sample was 0.23. More detailed information can be found in Wardlaw and Taylor (1976). The experimental data are shown in Fig. 7. The IDC and MWC were fitted using a least-squares method. The parameters are listed in Table 5. The MDC and secondary scanning curves were predicted by the new model. The predictive curves are also shown in Fig. 7.

The predictive MDC is close to the measured data, as shown in Fig. 7. One drying scanning curve was adopted to calibrate parameter d. Then, the other scanning drying and wetting curves were predicted by the model. The conformity of the drying scanning curves compared well with the measured data. Some deviations existed between the predictive curves and the measured data. The main reason for this is that the fitting result did not fit the MWC well when the matric suction was at low values. On the whole, as long as the previously experienced maximum matric suction was given, the new model was capable of modeling any change of the degree of saturation of mercury in the hysteretic loop determined uniquely by $s_{ci}^{\max}$. Therefore, it can be stated that the relationship between the pressure and degree of saturation of mercury in the rocks was significantly affected by entrapped mercury or air.

The distribution of pores is generally inhomogeneous and their connectivity is perplexing in unsaturated porous media (Frydman and Baker 2009). The phenomenon of capillary hysteresis and entrapped air in these media will commonly occur under intermittent

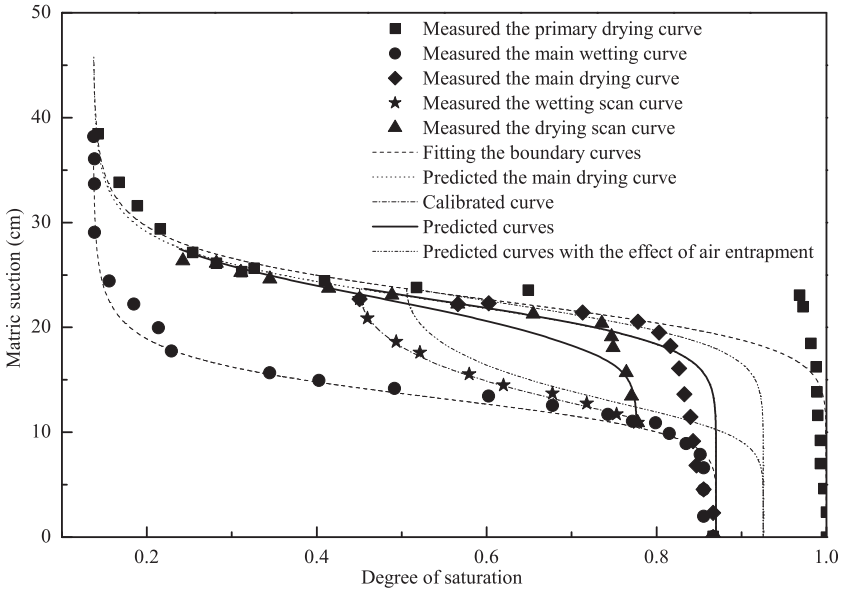

Fig. 6. Soil-water retention relationship of fine silica sand with the effect of entrapped air subjected to wetting-drying cycles

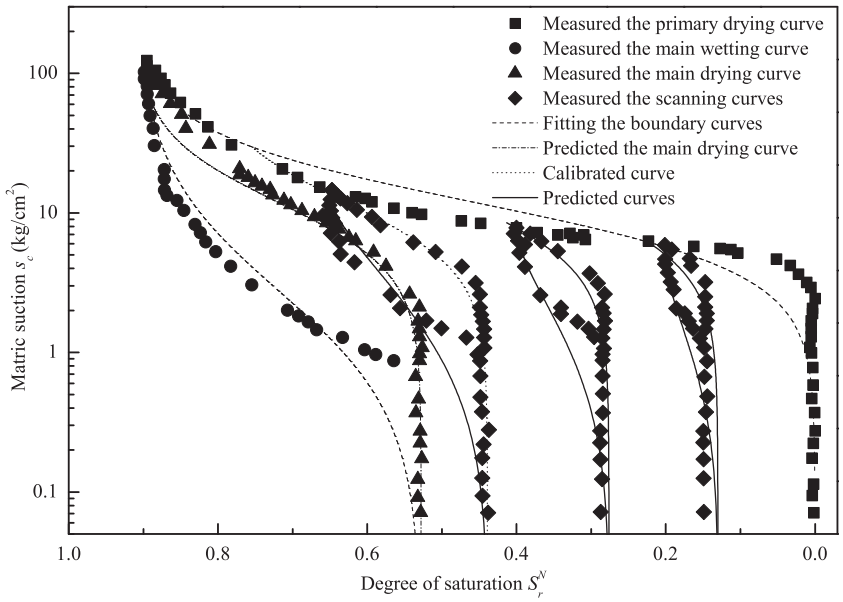

Fig. 7. Mercury injection and withdrawal cycled curves of Midale dolomite with the effect of entrapped mercury

rainfall infiltration and fluctuations in water table conditions. Hence, the two effects should be considered when modeling the soil-water retention relationship and unsaturated seepage problems under repeated changes of soil-water states. The predictive curves will be able to accurately describe the evolvement of the degree of saturation and matric suction.

Conclusions

Based on the analysis of the effect of capillary hysteresis and air entrapment in porous media, a new soil-water retention theoretical model has been developed that considers the effect of air entrapment on pore flow. The simple ISVH-trap model can predict well the

Table 5. Material Properties and Model Parameters of Midale Dolomite

Parameter	Symbol	Quantity	Unit
Porosity	n_0	0.23	—
Residual degree of saturation	S_r^{irr}	9.0	Percentage
Maximum degree of saturation of entrapped air	$S_{r\max}^{\text{trap}}$	52.8	Percentage
Model parameters for simple ISVH-trap	b^{IDC}	11.864	kg/cm^2
	b^{MWC}	2.767	kg/cm^2
	a^{IDC}	1.72	—
	a^{MWC}	0.96	—
	d	400	kg/cm^2

change of the soil-water state under arbitrary changes of hydraulic paths in unsaturated porous media. Only a few parameters are needed and the predictive method is easily implemented.

The proposed model was used to predict the soil-water retention relationship of an unsaturated porous medium subjected to complex drying-wetting cycles. By comparing the predictive curves with the measured data, the change of matric suction and the degree of saturation of the water phase in the unsaturated porous medium was significantly affected by the effect of entrapped air. The model with capillary hysteresis and air entrapment effects should be taken into account in the soil-water retention relationship in order to accurately predict the change of the soil-moisture state in a porous medium. The simulated results also show that as long as the previously experienced maximum matric suction $s_{ci}^{\max}$ or reversal degree of saturation S_r^{Wt} is given, the new model is capable of modeling any change of matric suction and degree of saturation of the water or air phase in the hysteretic loop determined uniquely by $s_{ci}^{\max}$.

Acknowledgments

The research is supported by the National Natural Science Foundation of China (Grant No. 11302243 and 11372078) and the Major Program of the National Natural Science Foundation of China (Grant No. 51239010).

Notation

The following symbols are used in this paper:

a, b = empirical parameters;
a^{IDC}, b^{IDC} = parameters by fitting the primary drying curve;
a^{MWC}, b^{MWC} = parameters by fitting the main wetting curves;
d = fit parameter to describe the scanning curves in the main hysteretic cycle;
G_s = specific gravity of soil particles;
K_p = slope of the scanning curve;
$\overline{K}_p$ = slope of the main drying and wetting boundary curves;
$\hat{n}$ = direction of the hydraulic path;
n_0 = porosity of samples;
r_i = equivalent radius of pores in the porous medium;
$r(S_r^W)$ = difference of the matric suction between the main boundary curves;
r_1 = equivalent radius of one type of pores in the porous medium;
r_2 = equivalent radius of another type of pores in the porous medium;
S_r^i = degree of saturation of the primary drying and main wetting curves with zero matric suction;
S_r^{IDC} = degree of saturation on the primary drying curve;
S_{ri}^{IDC} = degree of saturation of one point on the primary drying curve;
S_r^{irr} = residual degree of saturation of the water phase;
S_r^{MDC} = degree of saturation on the main drying curve according to $s_{ci}^{\max}$;
S_{ri}^{MDC} = degree of saturation of one point on the main drying curve;
S_r^{MHL} = degree of saturation in the main hysteretic loop at matric suction $(s_c + \dot{s}_c)$;
S_{ro}^{MHL} = degree of saturation in the main hysteretic loop at matric suction s_c;
S_r^{MWC} = degree of saturation with zero matric suction on the main wetting curve;
S_r^N = degree of saturation of nonwetting liquids;
S_r^{trap} = degree of saturation of entrapped air and entrapped dense nonaqueous phase liquid;
$S_{r\max}^{\mathrm{trap}}$ = maximum degree of saturation of entrapped air;
S_r^W = present degree of saturation in the main hysteretic loop and degree of saturation of the wetting liquid;
$\dot{S}_r^W$ = change of degree of saturation in the main hysteretic loop;
S_e^{Wt} = effective degree of saturation of water according to S_r^{Wt};
S_r^{Wt} = degree of saturation according to previous maximum matric suction;
s_c = present matric suction in the main hysteretic loop;
$\dot{s}_c$ = increment of matric suction;
$\overline{s}_c$ = matric suction in the main drying or wetting boundary curves;
s_c^C = matric suction on the Point C;
s_c^D = matric suction on Point D;
s_c^F = matric suction on Point F;
s_c^I = matric suction on Point I;
s_{ci} = matric suction on a point;
$s_{ci}^{\max}$ = previous maximum matric suction;
s_{c1} = matric suction according to r_1;
s_{c2} = matric suction according to r_2;
$\overline{s}_c(S_r^W, \hat{n})$ = matric suction of the main drying and wetting boundary curves;
$\kappa_D(S_r^W)$ = matric suction in the main drying boundary curves;
$\kappa_W(S_r^W)$ = matric suction in the main wetting boundary curves; and
ρ_d = dry density of samples.

References

Bond, W. J., and Collis-George, N. (1981). "Ponded infiltration into simple soil systems: 1. The saturation and transition zones in the moisture content profiles." *Soil Sci.*, 131(4), 202–209.

Chen, P., Wei, C., Liu, J., and Ma, T. (2013). "Strength theory model of unsaturated soils with suction stress concept." *J. Appl. Math.*, 2013, 756854.

Feng, M., and Fredlund, D. G. (1999). "Hysteretic influence associated with thermal conductivity sensor measurements." *Proc., 52nd Canadian Geotechnical and Unsaturated Soil Group Conf.: From Theory to the Practice of Unsaturated Soil Mechanics*, BiTech Publishers, Richmond, BC, Canada, 651–657.

Frydman, S., and Baker, R. (2009). "Theoretical soil-water characteristic curves based on adsorption, cavitation, and a double porosity model." *Int. J. Geomech.*, 10.1061/(ASCE)1532-3641(2009)9:6(250), 250–257.

Gerhard, J. I., and Kueper, B. H. (2003). "Relative permeability characteristics necessary for simulating DNAPL infiltration, redistribution, and immobilization in saturated porous media." *Water Resour. Res.*, 39(8), 1–16.

Gerhard, J. I., Kueper, B. H., and Hecox, G. R. (1998). "The influence of waterflood design on the recovery of mobile DNAPLs." *Ground Water*, 36(2), 283–292.
Hammecker, C., Antonino, A. C. D., Maeght, J. L., and Boivin, P. (2003). "Experimental and numerical study of water flow in soil under irrigation in northern Senegal: Evidence of air entrapment." *Eur. J. Soil Sci.*, 54(3), 491–503.
Hilpert, M., McBride, J. F., and Miller, C. T. (2000). "Investigation of the residual–funicular nonwetting-phase-saturation relation." *Adv. Water Resour.*, 24(2), 157–177.
Kechavarzi, C., Soga, K., and Illangasekare, T. H. (2005). "Two-dimensional laboratory simulation of LNAPL infiltration and redistribution in the vadose zone." *J. Contam. Hydrol.*, 76(3–4), 211–233.
Khoury, N., Brooks, R., Khoury, C., and Yada, D. (2012). "Modeling resilient modulus hysteretic behavior with moisture variation." *Int. J. Geomech.*, 10.1061/(ASCE)GM.1943-5622.0000140, 519–527.
Krishnapillai, S. H., and Ravichandran, N. (2012). "New soil-water characteristic curve and its performance in the finite-element simulation of unsaturated soils." *Int. J. Geomech.*, 10.1061/(ASCE)GM.1943-5622.0000132, 209–219.
Land, C. S. (1968). "Calculation of imbibition relative permeability for two- and three-phase flow from rock properties." *Soc. Pet. Eng. J.*, 8(2), 149–156.
Lenhard, R. J., Oostrom, M., and Dane, J. H. (2004). "A constitutive model for air–NAPL–water flow in the vadose zone accounting for immobile, non-occluded (residual) NAPL in strongly water-wet porous media." *J. Contam. Hydrol.*, 71(1–4), 261–282.
Lenhard, R. J., and Parker, J. C. (1987). "A model for hysteretic constitutive relations governing multiphase flow: 2. Permeability-saturation relations." *Water Resour. Res.*, 23(12), 2197–2206.
Likos, W. J., and Lu, N. (2002). "Hysteresis of capillary cohesion in unsaturated soils." *Proc., 15th ASCE Engineering Mechanics Conf.*, ASCE, New York, 1–8.
Likos, W. J., and Lu, N. (2004). "Hysteresis of capillary stress in unsaturated granular soil." *J. Eng. Mech.*, 10.1061/(ASCE)0733-9399(2004)130:6(646), 646–655.
Liu, C., and Muraleetharan, K. K. (2012). "Coupled hydro-mechanical elastoplastic constitutive model for unsaturated sands and silts. I: Formulation." *Int. J. Geomech.*, 10.1061/(ASCE)GM.1943-5622.0000146, 239–247.
Miller, C. T., Poirier-McNeill, M. M., and Mayer, A. S. (1990). "Dissolution of trapped nonaqueous phase liquids: Mass transfer characteristics." *Water Resour. Res.*, 26(11), 2783–2796.
Miller, G. A., Khoury, C. N., Muraleetharan, K. K., Liu, C., and Kibbey, T. C. G. (2008). "Effects of soil skeleton deformations on hysteretic soil water characteristic curves: Experiments and simulations." *Water Resour. Res.*, 44(5), W00C06.
Mohamed, M. H., and Sharma, R. S. (2007). "Role of dynamic flow in relationships between suction head and degree of saturation." *J. Geotech. Geoenviron. Eng.*, 10.1061/(ASCE)1090-0241(2007)133:3(286), 286–294.
Noh, J.-H., Lee, S.-R., and Park, H. (2012). "Prediction of cryo-SWCC during freezing based on pore-size distribution." *Int. J. Geomech.*, 10.1061/(ASCE)GM.1943-5622.0000134, 428–438.
Nuth, M., and Laloui, L. (2008). "Advances in modelling hysteretic water retention curve in deformable soils." *Comput. Geotech.*, 35(6), 835–844.
Parker, J. C., and Lenhard, R. J. (1987). "A model for hysteretic constitutive relations governing multiphase flow: 1. Saturation-pressure relations." *Water Resour. Res.*, 23(12), 2187–2196.
Poulovassilis, A. (1970a). "Hysteresis of pore water in granular porous bodies." *Soil Sci.*, 109(1), 5–12.
Poulovassilis, A. (1970b). "The effect of the entrapped air on the hysteresis curves of a porous body and on its hydraulic conductivity." *Soil Sci.*, 109(3), 154–162.
Seymour, R. M. (2000). "Air entrapment and consolidation occurring with saturated hydraulic conductivity changes with intermittent wetting." *Irrig. Sci.*, 20(1), 9–14.
Sharma, R. S., and Mohamed, M. H. A. (2003). "An experimental investigation of LNAPL migration in an unsaturated/saturated sand." *Eng. Geol.*, 70(3–4), 305–313.
Steffy, D. A., Johnston, C. D., and Barry, D. A. (1998). "Numerical simulations and long-column tests of LNAPL displacement and trapping by a fluctuating water table." *J. Contam. Hydrol.*, 7(3), 325–356.
Stegemeier, G. L. (1977). "Mechanism of entrapment and mobilization of oil in porous media." *Improved oil recovery by surfactant and polymer flooding*, D. O. Shah and R. S. Schechter, eds., Academic, New York, 55–91.
Stonestrom, D. A., and Rubin, J. (1989). "Water content dependence of trapped air in two soils." *Water Resour. Res.*, 25(9), 1947–1958.
Tan, Y.-C., Ma, K.-C., Chen, C.-H., Ke, K.-Y., and Wang, M.-T. (2009). "A numerical model of infiltration processes for hysteretic flow coupled with mass conservation." *Irrig. Drain.*, 58(3), 366–380.
Van Geel, P. J., and Roy, S. D. (2002). "A proposed model to include a residual NAPL saturation in a hysteretic capillary pressure–saturation relationship." *J. Contam. Hydrol.*, 58(1–2), 79–110.
Van Geel, P. J., and Sykes, J. F. (1997). "The importance of fluid entrapment, saturation hysteresis and residual saturations on the distribution of a lighter-than-water non-aqueous phase liquid in a variably saturated sand medium." *J. Contam. Hydrol.*, 25(3–4), 249–270.
Wardlaw, N. C., and Taylor, R. P. (1976). "Mercury capillary pressure curves and the interpretation of pore structure and capillary behaviour in reservoir rocks." *Bull. Can. Petrol. Geol.*, 24(2), 225–262.
Wei, C., and Dewoolkar, M. M. (2006). "Formulation of capillary hysteresis with internal state variables." *Water Resour. Res.*, 42(7), W07405.